J. Phys. B: At. Mol. Phys. **18** (1985) 2993-3009. Printed in Great Britain

An improved crossed-beams technique for the measurement of absolute cross sections for electron impact ionisation of ions and its application to Ar^+ ions†

A Müller‡, K Huber‡, K Tinschert‡, R Becker§ and E Salzborn‡

‡ Institut für Kernphysik, Universität Giessen, D-6300 Giessen, West Germany
§ Institut für Angewandte Physik, Universität Frankfurt, D-6000 Frankfurt, West Germany

Received 17 December 1984

Abstract. Based on the animated-beam method of Brouillard and co-workers an improved experimental technique has been developed to measure cross sections for electron impact ionisation of ions. In a crossed-beams arrangement the overlap of the electron and the ion beam is periodically varied by a mechanical displacement of the complete electron gun system. Simultaneously with the ionisation signal, the parent ion beam current and the velocity of the gun movement are registered. As a test of the new method cross sections for single ionisation of Ar^+ ions are measured from threshold up to 850 eV electron energy. The results are in excellent agreement with the crossed-beams data of Woodruff *et al.*

1. Introduction

The experimental investigation of electron impact ionisation of ions has revealed important new aspects of electron-ion interaction. Significant contributions of excitation-autoionisation processes to the ejection of a single electron (Falk *et al* 1981) and of inner-shell ionisation-autoionisation processes to multiple ionisation (Müller and Frodl 1980) have been observed. With increasing charge state of the ions these indirect mechanisms often tend to dominate the direct ionisation processes (Achenbach *et al* 1984).

In principle the measurement of total cross sections allows direct identification of contributing multi-step processes from structures in the cross section function which occur when the electron energy corresponds to the threshold of the indirect process. A good relative accuracy of the measurements is required for the identification of small irregularities in the cross sections and their attribution to the onset of new contributions. Since electron impact ionisation of ions is also of fundamental importance in understanding plasmas and is difficult to predict from first principles there is an immediate practical interest in accumulating experimental knowledge about features and trends in the cross sections. An absolute accuracy within ±10% would be desirable for data used in plasma modelling calculations.

Because of the general interest in the field and the inherent data needs we have considerably improved the experimental method used for our previous investigations of electron impact ionisation. With our new technique it is possible for each ionisation

† Work supported by Deutsche Forschungsgemeinschaft.

cross section measurement to be independently absolute. The data are accumulated by a computer which directly yields the resulting cross section with the statistical error and the total uncertainty. It is thus possible to obtain data with good accuracy in a relatively short time if the ion source provides the desired ions in sufficient quantity.

The new technique is based in principle on a method first described by Defrance *et al* (1981). This alternative method of cross section measurement involves sweeping one of the beams across the other in a linear motion. The method has several advantages compared with the ordinary crossed-beams technique employing modulation of beam intensities (Harrison 1968). It does not require a separate measurement of the form factor which describes the overlap of two intersecting static beams and, furthermore, since both beams are always 'on', background pressure modulation effects cannot occur.

We have applied the animated-beam principle (Brouillard and Claeys 1983) in the following way: an intense ribbon electron beam is moved mechanically up and down across an ion beam at a constant speed. The amplitude of the displacement is large enough to produce no overlap of the beams in the extreme positions. This gives a convenient way to measure the background events due to gas-stripping collisions. The number of accumulated signal counts obtained in the overlap region is directly proportional to the ionisation cross section and to the total intensities of both beams, no matter how these intensities are distributed spatially across the beams. The current of the parent ion beam and the actual speed of the motion are registered as a function of electron beam position simultaneously with the ionised-ion count rate. It is thus possible to obtain correct normalisation of accumulated signal counts to accumulated parent ion charge.

We have applied the technique to the measurement of the cross section $\sigma_{1,2}$ for electron impact single ionisation of Ar^+ ions in the energy range from threshold up to 850 eV. The results are compared with data of Woodruff *et al* (1978) which are generally considered accurate to within an absolute uncertainty of less than ±10%.

2. Method

When collimated electron and ion beams intersect at an angle θ, the rate R of ionised ions is given by

$$R = \sigma I_e I_i M / F \tag{1}$$

with

$$M = \frac{(v_e^2 + v_i^2 - 2v_e v_i \cos\theta)^{1/2}}{qe^2 v_e v_i \sin\theta} \tag{2}$$

and the form factor

$$F = I_e I_i \left(\int_{-\infty}^{+\infty} i_e(z) i_i(z)\, dz \right)^{-1} \tag{3}$$

where σ is the ionisation cross section, I_e and I_i are the total electric currents in both beams, q is the charge state of the parent ions, e is the charge of an electron and v_e and v_i are the velocities of the electrons and the ions, respectively. $i_e(z)\,dz$ and $i_i(z)\,dz$ are the differential currents of electrons and ions, respectively, in the interval in height

between z and $z+\mathrm{d}z$:

$$i_e(z) = \int_{-\infty}^{+\infty} j_e(y, z)\,\mathrm{d}y \tag{4a}$$

$$i_i(z) = \int_{-\infty}^{+\infty} j_i(x, z)\,\mathrm{d}x \tag{4b}$$

where $j_e(y, z)$ and $j_i(x, z)$ are the current densities of the electron and ion beams, respectively, in a plane perpendicular to the direction of that beam. The vertical coordinate perpendicular to both beams is z.

Consider now an ion beam consisting of only one beam slice of differential height $\mathrm{d}z$ with a total ion current $I_i = i_i(z)\,\mathrm{d}z$ crossing the electron beam at position z. In this case equation (1) reduces to

$$\mathrm{d}R(z) = \sigma M i_e(z) I_i. \tag{5}$$

In our previous investigations (Müller *et al* 1980, Achenbach *et al* 1984) we made use of equation (5) to determine ionisation cross sections with extremely collimated ion beams of a height very much smaller than the vertical extension of the electron beam with constant electron current density in the region of the crossing ion beam. The disadvantage of this former method rests in the assumption that the experimental $\mathrm{d}z$ was small enough to justify the application of equation (5) and in the difficulty of determining $i_e(z)$ and $i_i(z)$ in an independent measurement. The method employed to overcome these problems follows the proposal of Defrance *et al* (1980).

When the whole electron beam is swept at constant speed u across a segment of the ion beam (current $i_i(z)\,\mathrm{d}z$, height $\mathrm{d}z$), with the extreme positions z_1 and z_2 completely including the beams' interaction region, then the number $\mathrm{d}N$ of ionised ions produced during one sweep is given by

$$\begin{aligned}\mathrm{d}N &= \int \mathrm{d}R(z')\,\mathrm{d}t = \int_{z_1}^{z_2} \frac{\mathrm{d}R(z')\,\mathrm{d}z'}{u} \\ &= \sigma M \frac{i_i(z)\,\mathrm{d}z}{u} \int_{z_1}^{z_2} i_e(z')\,\mathrm{d}z' \\ &= \sigma M i_i(z)\,\mathrm{d}z\, I_e/u.\end{aligned} \tag{6}$$

A real ion beam with the total electric current I_i is composed of differential beam elements of height $\mathrm{d}z$ with current $i_i(z)\,\mathrm{d}z$. When the electron beam is moved completely across the whole ion beam the total number of ionised ions per sweep is

$$\begin{aligned}N &= \sigma M (I_e/u) \int_{z_1}^{z_2} i_i(z)\,\mathrm{d}z \\ &= \sigma M I_e I_i/u.\end{aligned} \tag{7}$$

Thus σ can be determined from an accumulated number N of ionised ions, the total electric currents I_e and I_i of electrons and ions respectively, the velocity u of the movement and the factor M, which depends only on the particle velocities in both beams, the angle of crossing, and the charge state of the parent ions.

3. Apparatus

3.1. General

Figure 1 shows a schematic view of the apparatus. The present arrangement is based on the set-up used previously by Müller *et al* (1980) and Achenbach *et al* (1984).

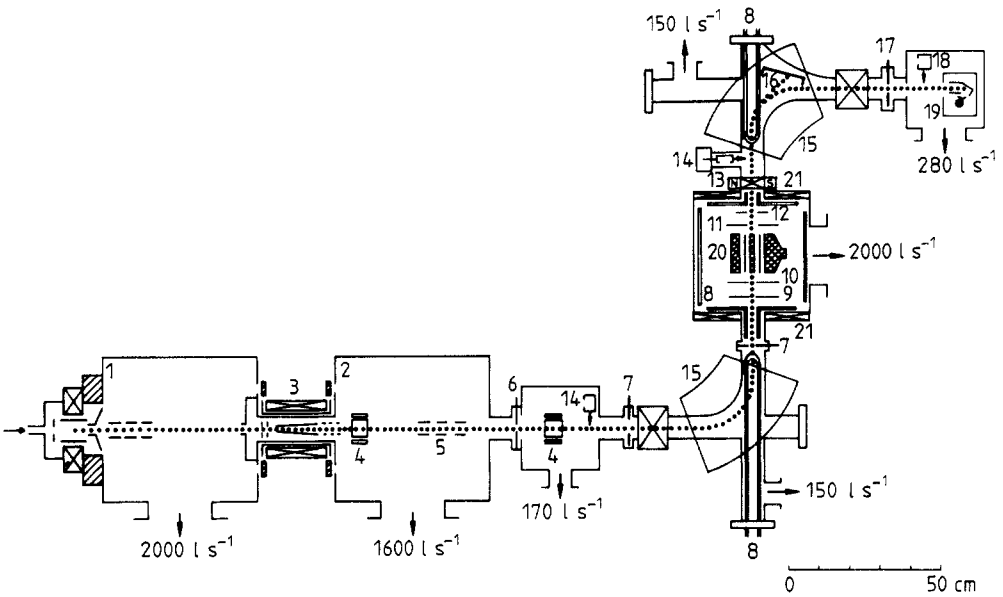

Figure 1. Schematic view of the total experimental set-up: 1, vacuum tank with Penning ion source and ion extraction system; 2, vacuum tank with electric steerer plates (4) and einzel lens (5); 3, electron beam ion source; 6, iris aperture; 7, rectangular apertures of variable diameter and position; 8, liquid-N_2-cooled copper plates; 9, 10, 11, wheels with 20 different combinations of apertures for probing and collimating the ion beam; 12, 17, iris apertures; 13, steering magnet; 14, 18, moveable Faraday cups; 15, analysing magnets; 16, large-acceptance Faraday cup; 19, single-particle detector; 20, electron gun mounted on a goniometer; 21, Helmholtz coils.

Multiply charged ions can either be produced by an electron beam ion source (Clausnitzer *et al* 1975, Müller and Salzborn 1979) or by a cold-cathode Penning ion source (Baumann and Bethge 1981). Ions can be extracted continuously from either source and accelerated to ground potential by a voltage of typically 10 kV. Four pairs of electric field plates and an einzel lens are used to steer and focus the ion beam. A 90° double focusing magnet separates the ions into beams of given charge and mass. An iris aperture and two rectangular apertures with size and position adjustable from outside the vacuum serve to regulate the intensity of the incident ion beam before it enters the collimator in front of the crossing electron beam. The collimator consists of two apertures mounted on two wheels 36 mm apart from each other with the axis of rotation parallel to the ion beam. By rotating the wheels it is possible to move different pairs of apertures into the ion beam line without breaking the vacuum. Aperture combinations used for cross section measurements are between 0.2 mm diameter and 0.7 mm diameter for each aperture. Parent and product ion beam

diameters can be controlled by an iris aperture downstream of the interaction region, and 100% transmission of both beams to their detectors can be assured experimentally.

A second 90° double focusing magnet serves for separation of parent and product ions. The ionised ions are directed into a single-particle detector (Rinn *et al* 1982), the parent ion beam is collected by a large Faraday cup (effective surface: 2 cm × 25 cm) mounted inside the second magnet chamber. The diameter of the iris aperture in front of the single-particle detector (effective surface: 20 mm ∅) can be varied to ensure complete collection of ions. Faraday cups before and behind the second magnet can be moved into the beam line for beam adjustment and transmission measurements.

The vacuum chamber housing the interaction region is pumped by a 2000 l s^{-1} oil diffusion pump; the magnet chambers are each pumped by 150 l s^{-1} oil diffusion pumps. All flanges on the magnet chambers and the interaction chamber have metal seals. Copper plates cooled by direct liquid-nitrogen flow are installed inside these chambers. After baking the apparatus to about 150 °C and pumping the liquid nitrogen through the cooling system the following pressures are reached: 2×10^{-9} mbar in the magnet chambers and 3.5×10^{-10} mbar in the interaction chamber.

3.2. The interaction region

For realising the method of cross section measurements described in § 2 the electron gun used in our previous experiments had to be modified, though the principle of a high-intensity electron beam of high perveance was maintained in order to provide high ionisation rates. The new device is schematically shown by the perspective view in figure 2. The electron beam extends 60 mm in the ion beam direction. Electrons are emitted from a curved cathode made of impregnated tungsten. The arrangement

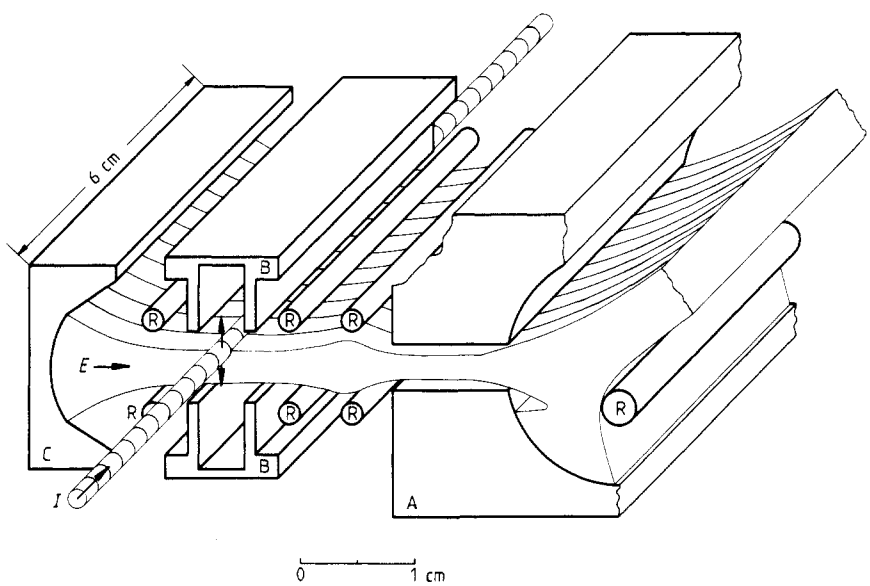

Figure 2. Perspective view of the electron gun with the ion beam crossing the interaction region. In the frame of the electron gun the ion beam moves up and down in the z direction. C, cathode; R, rod electrodes; B, rectangular electrode defining the displacement region; A, anode; E, electron beam; I, ion beam.

of six rod electrodes and a central rectangular tube at proper voltages define the electric potential distribution and the electron trajectories such that the requirements for the application of equation (7) can be met. After crossing the beams' interaction region the electron beam enters a slit in the anode collector and is then defocused by a rod electrode mounted off-centre within the cylindrical bore. Thus the power transported by the electron beam (370 W at an electron energy of 1000 eV) is dissipated onto a large surface and there is little chance for an electron to travel back to the interaction zone and contribute again to ionisation. The collector is made from a solid copper block and is directly cooled by flowing water.

The electron gun is mounted on a vacuum manipulator which allows the gun to move up and down across the ion beam. The movement is driven by a DC electric motor. The position of the gun is measured by a potentiometer circuit. The voltage provided by the potentiometer is also used to switch off the motor in its end positions, which can be preset by a control unit.

The design of the electron gun is based on computer calculations of the potential distribution and electron trajectories in a given electrode arrangement. In the calculations the space charge of charged particles is taken into account as well as the thermal energy spread of the electrons emitted from the cathode surface. Equipotential lines and representative electron trajectories calculated for the present electron gun are shown in figure 3 in a plane perpendicular to the ion beam. The electric potentials applied to the different electrodes are given in per cent of the maximum voltage U_{max}. The position of the ion beam is marked by the stippled circular section. When the gun is moved in the z direction beginning from an extreme position about 9 mm from the ion beam axis, the ion beam first hits the rectangular electrode resulting in no ion transmission to the detectors. Then the ion beam crosses the gun in a region free of interaction with the electron beam so that only collisions with residual gas particles occur. Such collisions give the dominant fraction of background events registered in the single-particle detector. When both beams intersect, the detector signal increases by the rate of ionised ions produced, and at the other side of the electron beam again only background is measured until the ion beam hits the opposite electrode.

A basic condition for doing measurements with the procedure described is a *constant* electric potential in the whole area where the ion beam can cross the electron gun, so

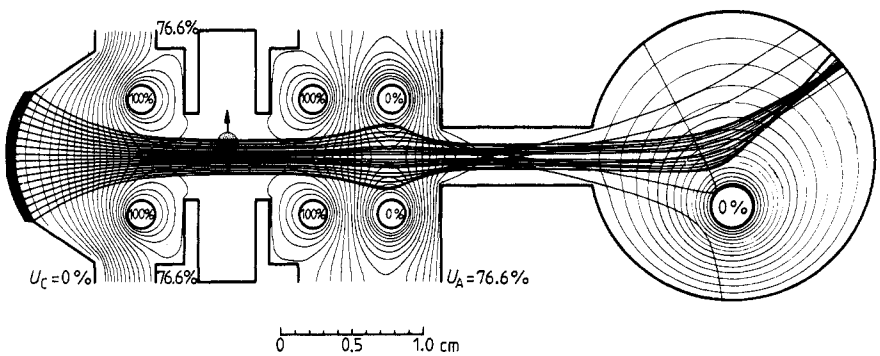

Figure 3. Calculated equipotential lines and electron trajectories of the electron gun in a plane perpendicular to the ion beam direction; the stippled area marks the ion beam section. The electric potentials applied to the electrodes are given in per cent of the maximum voltage U_{max}. The equipotentials are at 5% intervals.

that the ion beam is not deflected. A constant electric potential in the region of electron-ion interaction is also required for a well defined electron energy. In order to achieve this the rectangular box electrode with a voltage of $0.766\,U_{max}$ was installed instead of another rod electrode used in the preceding gun (see Achenbach *et al* 1984). The density of equipotential lines calculated for the present electron gun (see figure 3) indicates that inside the box where the ion beam crosses there is no, or at most a weak, potential gradient. The measurements show that the parent ion beam is not deflected during the movement of the electron gun: the calculated potential differences within the electron beam do not exceed ±2% of the potential applied to the rectangular box electrode. The space charge of the electrons may be compensated, however, by slow ions produced from residual gas atoms. In the case of complete compensation there is a completely uniform electric potential in the whole interaction region with the electron energy exactly defined. The slow ions will become trapped by the electron beam and the possibility of ionisation of the incident ion beam by these trapped ions must be considered (see § 6).

4. Experimental procedure

The magnetically analysed beam of ions with charge state $q_{initial}$ is collimated in front of the electron gun to a maximum diameter of 2 mm. The product ions with charge state q_{final} produced by electron impact ionisation or by collisions in the residual gas are directed into the single-particle detector. At the same time the parent ions are collected by the large Faraday cup inside the second magnet chamber. Since this cup is 25 cm wide it is possible to measure the product ion flux and the parent ion current simultaneously for different charge state ratios $q_{initial}/q_{final}$ without moving the cup and breaking the vacuum.

Figure 4 shows the detector signal obtained with Ar^{2+} ions produced from parent Ar^+ ions as a function of the analysing magnetic induction B. The ions have an energy

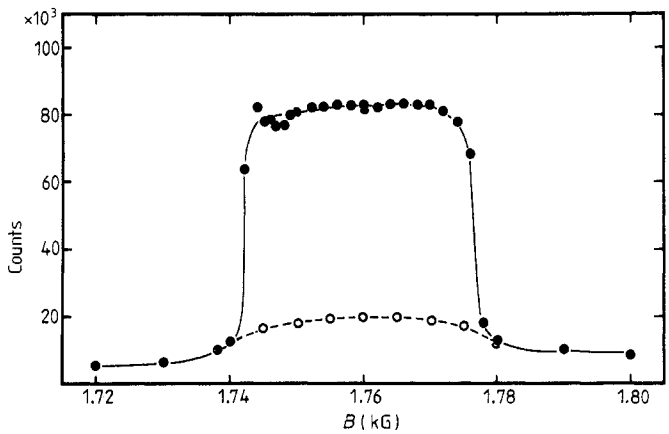

Figure 4. Signal of the single-particle detector as a function of the magnetic field of the second analysing magnet. The detector pulses were accumulated until the parent-ion-beam Faraday cup (figure 2, item 16) had collected a given charge. The full circles indicate measurements of electron impact ionisation plus background (both beams overlap) while the open circles indicate background measurements only (beams did not overlap).

of 10 keV and traverse the electron gun with an electron beam energy of 100 eV. In a position where the two beams do not intersect, the measured signal is indicated by the open points connected by a broken curve to guide the eye. In a second position of the electron gun where both beams overlap there is obviously additional signal arising from electron impact ionisation. The observed peak rises and falls abruptly and is 'flat topped', indicating that all product ions—at least those arising from electron impact—are collected by the detector. The small irregularities on the flat top of the peak are larger than the statistical uncertainty and are probably due to small deviations from a uniform detection efficiency. For cross section measurements the magnetic field is set to the centre of the product ion peak.

The electron gun can now be moved up and down between two extreme positions about ±9 mm from the ion beam axis. During the movement four multichannel analyser spectra are taken with an analogue-to-digital converter operating in the sampling mode. The signal to be sampled is the ramp voltage generated by the potentiometer which measures the actual position of the electron gun.

For the first spectrum this voltage is sampled by the pulses of the single-particle detector. Thus the rate of ionised ions can be obtained as a function of electron gun position z. The second spectrum is generated by sampling the ramp voltage with pulses from a current-to-frequency converter used in measuring the parent ion current. Thus the parent ion current is obtained as a function of z and of course this current has to be constant as long as the ion beam does not hit an electrode. The usual fluctuations in the ion beam intensity due to ion source operation are smoothed over by moving the gun up and down several times. One complete movement takes about 20 s. The third spectrum gives information about the velocity u of the movement. It is generated by sampling the ramp with pulses from a constant-frequency pulse source. Consider the ramp voltage is $V = \alpha z$ with a constant α, and the rate of sampling pulses is r_s with constant period r_s^{-1}. After one movement the number of counts Δn in one channel of width ΔV is

$$\Delta n = r_s \Delta t = r_s \Delta z / u = r_s \Delta V / \alpha u. \tag{8}$$

For ΔV infinitely small and constant for each channel, and α constant for all z, Δn is proportional to $1/u$. In the case that u is also constant each channel would have the same content. Thus in principle the three spectra discussed above could be directly used for the evaluation of cross sections. However, in reality there are some difficulties and limitations. The transfer of data from the experiment to the computer is limited in our case to 3000 pulses per second. Furthermore, there is a dead time mainly due to the analogue-to-digital converter (ADC) which has been measured to be about 30 μs.

The limitation of the overall pulse rate can be easily met by really offering less than 3000 pulses per second to the system by means of appropriate prescalers. Additionally an intermediate data buffer is used which stores pulses until they can be accepted by the transfer system. This is necessary when pulse intervals become too short due to statistical fluctuations in the production of ionised ions.

The loss of events due to the time τ of the pulse transfer system can also be compensated experimentally. Consider a rate r of pulses from a random source. The average number m of pulses falling within a dead-time interval τ is then given by $m = r\tau$. A dead-time interval starts when a pulse is registered. According to Poisson statistics the probability to have no further pulses during the time interval τ is $P_0 = e^{-m}$. With a maximum rate $r = 1000\ s^{-1}$ used in the present experiment m is equal to 0.03 giving a maximum fraction of pulse losses $1 - P_0 \simeq m = 0.03$. To avoid even this fraction

of loss a fourth spectrum is generated by which most of the losses can be compensated: when the ADC has just received one pulse it gives a 'busy' signal until it is ready to accept the next pulse. The incoming pulses are measured in coincidence with the 'busy' signal of the ADC and in case of a coincidence, i.e. when the time interval between two subsequent pulses is smaller than τ, then the coincidence pulse is stored in the fourth spectrum. By adding the fourth to the first spectrum possible pulse losses due to statistical fluctuations of the signal intensity are reduced to $1-P_0-P_1 \leqslant 5\times10^{-4}$ as long as r is less than or equal to $1000\,s^{-1}$. In general, spectrum 4 is completely empty since in most cases the prescalers reduce the original pulse rates to values which do not cause pile-up problems.

In our experiments each spectrum has a length of 490 channels resulting in a high-resolution measurement of the electron gun position. One channel corresponds to about $\frac{1}{30}$ of a millimetre. At this resolution fluctuations in the number Δn of counts in one channel may occur due to three effects. In addition to the source intensity statistics the voltage range ΔV for one ADC channel may vary with the channel number, and, furthermore, fluctuations in α (caused e.g. by an AC noise on the ramp voltage) may also lead to fluctuations in Δn. Nevertheless we used the high resolution for an accurate measurement of the extreme positions which directly enter into the final cross section formula (see § 5). The spectra can be easily smoothed by summation over groups of, for example 10 channels, reducing the total length to 49 channels. Fluctuations in α and ΔV are averaged in this case and it becomes obvious that parent ion current and speed of electron gun motion are constant within good accuracy.

Figure 5 shows a typical set of the first three spectra taken for the measurement of one cross section point. The investigated process is $e+Ar^+ \rightarrow Ar^{2+}+2e$ at an electron energy of 48 eV. Equation (8) makes clear that Δn for the channels which correspond to the end positions of the electron gun where the motion stops should go to infinity. This fact can be used for an accurate determination of the number of channels corresponding to the displacement $\Delta z = z_2 - z_1$ of the electron gun.

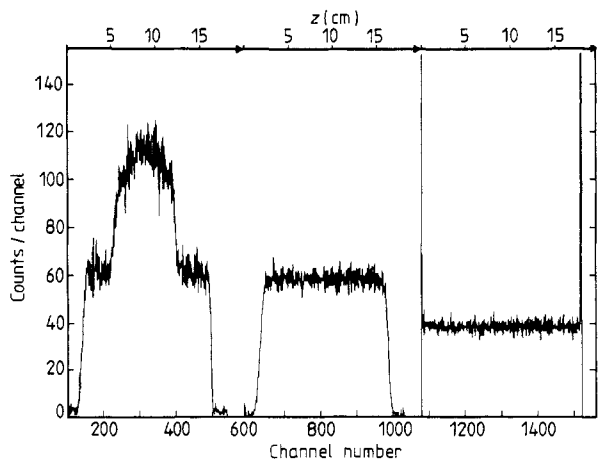

Figure 5. A typical set of three MCA spectra acquired at an electron energy of 48 eV showing (from left to right) the signals of the ionised ions, the parent ion current and the velocity of the electron gun movement as a function of electron gun position (respectively channel number).

5. Evaluation of cross sections

Ionisation cross sections are evaluated on the basis of equation (7). The first task is the determination of the real number of ionised ions N produced during the movement of the electron beam. For this purpose the background measured when there is no beam overlap has to be subtracted from the total signal obtained. It is assumed that the background is proportional to the ion beam intensity since the electron beam does not influence the single-particle detector.

The procedure of data evaluation is discussed for an idealised set of spectra shown in figure 6. The integration limits (channel numbers) L_1, L_3, L_4, L_6 are set by the experimenter to separate the background from the peak with the real ionisation signal.

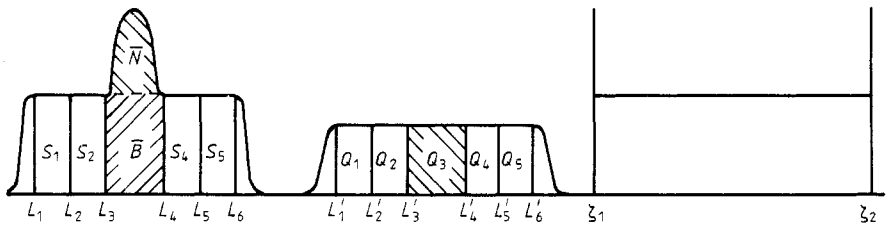

Figure 6. Idealised MCA spectra for the rate of ionised ions, the current of parent ions and the velocity signal as a function of electron gun position z. Integration limits and integrals used in the data evaluation (see test) are shown.

The following steps are done automatically by the computer. The limits L_2 and L_5 are set to the centre of the intervals (L_1, L_3) and (L_4, L_6), respectively. All these limits are correspondingly used also in the parent ion spectrum which has the same length as the product ion spectrum: $L_i \rightarrow L_i'$; $i = 1, \ldots, 6$. Integrals S_i and Q_i ($i = 1, \ldots, 5$) are calculated with

$$S_i = \sum_{m=L_i}^{L_{i+1}-1} \Delta n_m \qquad Q_i = \sum_{M=L_i'}^{L_{i+1}'-1} \Delta n_m \tag{9}$$

where Δn_m is the number of counts in channel m of the respective spectrum. The integrals S_i and the corresponding Q_i, which are proportional to collected parent ion charge, can be used to determine the average number of background counts per channel and per unit parent ion charge. Since $S_3 = \bar{S} = \bar{B} + \bar{N}$, the number of ionised ions $N = \bar{N}/\varepsilon$ (ε is the detector efficiency) can be expressed by

$$N\varepsilon = \bar{N} = \bar{S} - \bar{B} = S_3 - \tfrac{1}{4}Q_3(S_1/Q_1 + S_2/Q_2 + S_4/Q_4 + S_5/Q_5). \tag{10}$$

The ion charge collected in channels L_3' to $L_4' - 1$ during one move of the electron beam can be deduced from the conversion factor C of the current-to-pulse-rate converter measuring the parent ion current $I_i = CR_i$, where R_i is the pulse rate used to sample the ramp voltage for the second spectrum. C is typically 1 nA kHz^{-1}.

$$Q = Q_3 = \frac{I_i}{C}\Delta t' = \frac{I_i}{C}\frac{\Delta z'}{u} = \frac{I_i}{u}\frac{(L_4' - L_3')}{CK} \tag{11}$$

where $\Delta t'$ is the time the electron gun takes to travel across $\Delta z'$, which corresponds to the interval (L_3', $L_4' - 1$). K is the number that converts a length into a number of

channels. K is determined by a geometric measurement of the difference $\Delta z = z_2 - z_1$ between the end positions of the gun ($\Delta z = 17.2 \pm 0.1$ mm) and by a computer search for the 'poles' in the velocity spectrum which determines the channels ζ_1 and ζ_2:

$$K = (\zeta_2 - \zeta_1)/(z_2 - z_1) \tag{12}$$

The ratio I_i/u which enters equation (7) is determined from equation (11). As a consequence the velocity u of the electron gun movement does not explicitly enter the cross section formula and need not be measured directly. Since the crossing angle of the two beams is $\theta = 90°$, σ is determined from

$$\sigma = \frac{\bar{N} q e^2 v_e v_i (L_4' - L_3')}{I_e \varepsilon (v_e^2 + v_i^2)^{1/2} QKC}. \tag{13}$$

6. Sources of error

The most important parameter in equation (13) is the measured number of ionised ions $\bar{N}$. Since it is based on the counting of random events its mean has a statistical uncertainty which is evaluated for a 95% confidence level from

$$\left(\frac{\Delta \bar{N}}{\bar{N}}\right)_{\text{stat}} = \pm 2 \frac{(S_3 + \tilde{B}\Delta)^{1/2}}{S_3 - \tilde{B}\Delta} \tag{14}$$

with $\tilde{B} = S_1 + S_2 + S_4 + S_5$ and $\Delta = (L_4 - L_3)/(L_3 - L_1 + L_6 - L_4)$. The underlying assumption for this formula is that the average number of background counts per channel does not change during the movement of the electron gun. The factor Δ corrects for the different time invervals during which the signal peak and the real background are measured.

As in every other electron-ion crossed-beams experiment the electrons may ionise residual gas atoms or molecules and the resulting ions compensate the electron space charge if they are not specifically extracted from the electron beam. In the present experiment trapping of slow ions may occur, which makes a very uniform electric potential in the whole interaction region. However, this gives an additional target for the incident fast ions. Background arising from the resulting ion-ion collisions cannot be determined directly in the present experiment and therefore requires further consideration. Since the trapped-ion target is moved in the same way as the electron beam one obtains with the formalism of § 2 a number of ionised ions $N^{(i)}$ produced by ion-ion collisions

$$N^{(i)} = \sigma^{(i)} I_i I_e/(q e^2 v_e u) \tag{15}$$

where $\sigma^{(i)}$ is the cross section for ionisation of fast ions by slow trapped ions. For equation (15) the trapped-ion density was assumed equal to the electron density. Since $\sigma^{(i)}$ does not depend on the electron energy the number $N^{(i)}$ increases proportional to I_e/v_e or, since $I_e \sim E_e^{3/2}$, proportional to the electron energy E_e. Nevertheless the apparent ionisation cross section σ_{app} measured in the present experiment has the following dependence on the electron velocity

$$\sigma_{\text{app}} = \frac{(N + N^{(i)})u}{I_e I_i M} = \sigma + \sigma^{(i)} \frac{v_i}{(v_e^2 + v_i^2)^{1/2}}. \tag{16}$$

For an electron energy below the electron impact ionisation threshold the apparent cross section is only dependent on the ionisation cross section $\sigma^{(i)}$ of the ion–ion collisions. Equation (16) especially also shows that the deviation of σ_{app} from σ is largest when $v_e = 0$ and then decreases monotonically with increasing electron energy. Although the number of trapped ions increases with the electron energy and can reach high values in our high-density electron beam, equation (16) shows that the measured apparent cross section σ_{app} approaches σ with increasing E_e. When there is an apparent cross section below threshold, e.g. of order 1% of the maximum of σ as in the case of $e + Ar^+ \rightarrow Ar^{2+} + 2e$ (see § 8), the deviation between σ_{app} and σ can be neglected compared with the remaining uncertainties of the measurement, and becomes less important the higher the electron energy. In a case where σ_{app} would be high below threshold and the presence of metastable ions in the parent beam could be exluded, the trapped ions would have to be extracted from the electron beam—in this experiment as well as in any other electron–ion crossed-beams arrangement—to obtain accurate ionisation cross sections.

The determination of the correct value $\bar{N}$ can be complicated by fluctuations in the parent-ion intensity: the time for one move of the electron gun ($\simeq$20 s) is long compared with the times during which beam intensity fluctuations may occur. Although these fluctuations are averaged over by moving the electron beam several times up and down across the ion beam they still may affect the cross section measurement. When the ionisation signal is small compared with the background a small increase of the parent ion beam intensity and the resulting increase of background counts may lead to a spurious increase of the measured cross section. With an ideal ADC and correct definition of the electron beam position this problem might be easily solved by normalisation of the contents in each channel of the signal spectrum to the contents of the corresponding channels in the parent-ion intensity spectrum (see figure 5). Because of variations in the widths ΔV of the channels and electrical noise on the ramp voltage V this was not practicable in the present arrangement. In this experiment the normalisation is made for groups of channels, namely those included by the integration limits L_i and L_i' ($i = 1, \ldots, 6$). Thus fluctuation of the parent ion current can be partly taken into account. The remaining uncertainty is added to the total error. For an experimental approach to this uncertainty four cross sections are determined from each spectrum, each taking only one out of the four ranges of background into account. In principle all these ranges give equivalent information about the background. The four cross sections are determined from equation (13) with $\bar{N}$ replaced by $\bar{N}_i = S_3 - Q_3 S_i / Q_i$ ($i = 1, 2, 4, 5$). Two thirds of the maximum deviation from the average cross section determined from equation (13) is considered as a reasonable estimate of the uncertainty introduced by intensity fluctuations in the parent ion beam, by variations in the speed u of the electron gun movement or by spurious noise pulses occurring mostly due to perturbations in the electric power line. The uncertainty $\Delta\bar{N}/\bar{N}$ introduced by these effects only plays a role below or just at the threshold of the investigated electron impact ionisation cross section.

The factor M (see equation (2) with $\theta = 90°$) has an uncertainty of $\pm 1\%$ due to possible errors in the measurement of v_e and v_i, which are estimated to be accurate within $\pm 1\%$. The velocity v_i is determined by the setting and the resolution of the analysing magnet and v_e is calculated from the voltage applied to the rectangular box electrode inside the electron gun. According to the calculations of the electron gun potential distribution this voltage is equal to that inside the electron beam in the region where the ion beam can cross. The uncertainties in the determination of electron

current I_e and accumulated charge QC are directly related to the accuracy of the electrometer and the current-to-frequency converter used. These uncertainties are quoted to be within ±3% and were checked by a calibrated constant-current source. The detector efficiency ε is taken from measurements similar to those reported earlier (Rinn *et al* 1982): $\varepsilon = 0.97 \pm 0.03$. The error of the conversion constant K is determined by the absolute uncertainty of the displacement Δz and the uncertainty for the difference of corresponding channel numbers $(\zeta_2 - \zeta_1)$ which is of order $\frac{1}{500}$.

The relative errors of all parameters entering equation (13) are squared and then summed. The square root of the resulting sum is the probable relative overall uncertainty which is determined with a 95% confidence level for the statistical error.

7. Test measurements

The reliability of the present experimental technique was checked by the measurement of ionisation cross sections with different ion current intensities ranging from 10 pA to several nA. Within the fluctuations occurring due to the uncertainties discussed in § 6 the measured cross sections are constant.

For collisions $e + Ar^+ \rightarrow Ar^{2+} + 2e$ the cross sections at centre-of-mass energies of 57 and 390 eV were measured with the energy of the parent ions varied from 500 eV up to 16 keV. The results of these meaurements are displayed in figure 7. Only at the very low ion energies below 2 keV are real deviations from the average cross section values found. In general a constant voltage of 10 kV is used to accelerate the parent ions, which is high enough to ensure correct cross section measurements.

This statement also holds for ions in higher charge states q. When there are potential gradients inside the electron gun their influence on the ion beam increases linearly with q for a given ion energy. However, since the ions are accelerated from the ion source by a fixed voltage their energy is proportional to q which compensates for the increased influence of potential gradients.

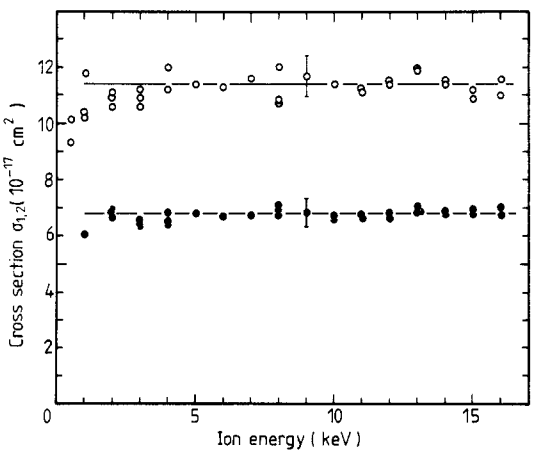

Figure 7. Dependence of the cross section on the ion energy at centre-of-mass energies of 57 eV (open circles) and 390 eV (full circles). The straight lines show the arithmetic mean value of all data points for one electron energy.

8. Results for single ionisation of Ar^+ ions

With the method described above, absolute cross sections were determined independently for single ionisation of Ar^+ ions in collisions

$$e + Ar^+ \rightarrow Ar^{2+} + 2e. \tag{17}$$

The resulting cross sections are shown in figure 8 together with measurements of Woodruff *et al* (1978). The two sets of data are in excellent agreement. Both cross sections rise from the threshold energy of 27.63 eV for ground-state ionisation of Ar^+ indicating that metastable ions do not play a role in the parent ion beam used. The reason might be that the Ar^+ ion does not have low-lying metastable states which could be populated in the ion source. (The metastable $^2P^o_{1/2}$ state with an excitation energy of only 0.18 eV is attributed to the ground state.) Zero signal below threshold also shows that there is no significant influence of a possible additional trapped-ion target (see equation (16)). The numerical results obtained in the present experiment are given in table 1 together with the total uncertainty including the statistical error at 95% confidence level.

Also shown in figure 8 are calculated cross sections $\sigma_{1,2}$ for process (17). The full curve is calculated from the simplified semi-empirical Lotz formula (Lotz 1968)

$$\sigma_{\text{Lotz}} = 4.5 \times 10^{-14}\ \text{cm}^2\ \text{eV}^2 \sum_i \frac{n_i \ln(E/P_i)}{EP_i} \tag{18}$$

where n_i is the number of electrons in the ith subshell and P_i the corresponding binding energy. E is the electron energy. For the present calculation we summed only over

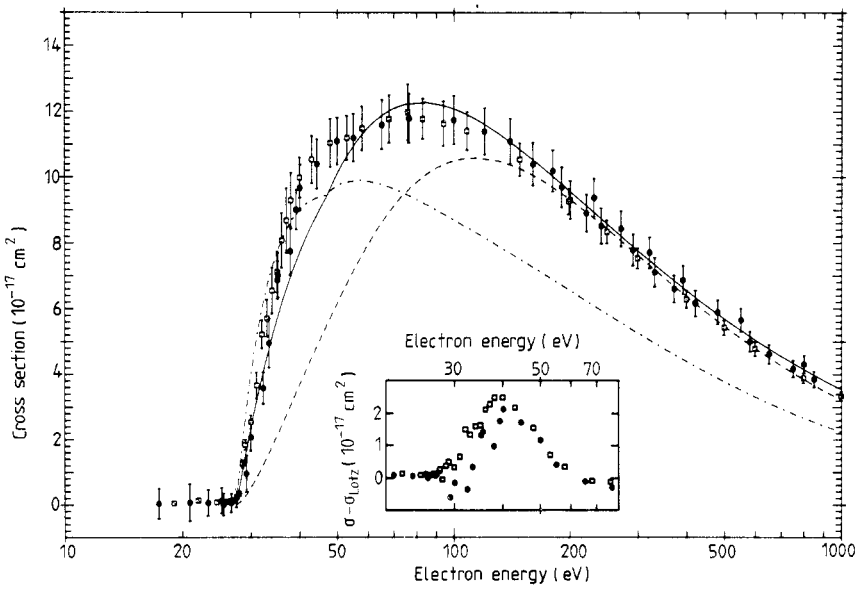

Figure 8. Cross sections $\sigma_{1,2}$ for $e + Ar^+ \rightarrow Ar^{2+} + 2e$. Full circles, present experiments; open squares, measurements by Woodruff *et al* (1978); full curve, semi-empirical Lotz cross section; chain curve, DWX calculation by Younger (1982); broken curve, semiclassical binary encounter approximation by Gryzinski (1965). The inset shows the difference between the experimental data points and the Lotz formula up to an electron energy of 80 eV.

Table 1. Electron impact ionisation cross sections $\sigma_{1,2}$ of Ar^+ ions. Estimated total uncertainties are given including the statistical error at 95% confidence level.

Electron energy (eV)	Cross section (10^{-17} cm^2)	Electron energy (eV)	Cross section (10^{-17} cm^2)
17.4	0.04 ± 0.46	139.8	11.1 ± 0.7
20.9	0.07 ± 0.57	160.0	10.4 ± 0.7
23.3	0.06 ± 0.38	180.0	10.2 ± 0.6
25.2	0.13 ± 0.39	190.0	9.70 ± 0.61
25.5	0.01 ± 0.34	200.0	9.31 ± 0.57
26.7	0.06 ± 0.29	220.0	8.91 ± 0.56
27.5	0.21 ± 0.29	230.0	9.38 ± 0.58
29.2	0.95 ± 0.56	240.0	8.52 ± 0.55
30.0	2.07 ± 0.42	270.0	8.44 ± 0.55
32.3	3.58 ± 0.49	290.0	7.79 ± 0.48
33.4	4.95 ± 0.75	320.0	7.71 ± 0.47
35.1	6.87 ± 0.58	330.0	7.11 ± 0.45
35.2	7.02 ± 0.68	370.0	6.61 ± 0.41
37.9	7.75 ± 0.74	390.0	6.87 ± 0.45
39.2	9.01 ± 0.60	420.0	6.17 ± 0.38
40.1	9.68 ± 0.71	479.0	5.90 ± 0.37
44.4	10.4 ± 0.8	550.0	5.66 ± 0.35
50.0	11.1 ± 0.7	580.0	5.00 ± 0.31
55.1	11.2 ± 0.7	650.0	4.62 ± 0.30
65.2	11.6 ± 0.8	750.0	4.17 ± 0.26
76.5	11.8 ± 0.8	800.0	4.31 ± 0.27
100.0	11.8 ± 0.7	850.0	3.85 ± 0.24
120.0	11.4 ± 0.7		

the 3p shell and the 3s shell since ionisation of the L shell predominantly leads to subsequent electron emission thus contributing only to multiple ionisation. The fluorescence yield of the L shell of Ar^+ is of order 10^{-3} (Chen and Crasemann 1974). For the binding energies we used $P_1 = 27.63$ eV for the 3p shell (Moore 1970) and $P_2 = 46.5$ eV for the 3s shell (Clementi and Roetti 1974). Good agreement with the experimental cross section is obtained; significant deviations only occur for electron energies between 35 and 55 eV. Around 40 eV the measured cross section shows a little structure which may be taken as a hint for an additional contribution to the single-ionisation cross section. This is supported by the form of $(\sigma_{exp} - \sigma_{Lotz})$ also displayed in figure 8 which was calculated with all experimental cross sections σ_{exp} from the two data sets. Younger (1982) pointed out that indirect single ionisation of chlorine-like ions, where ionisation proceeds via an autoionising resonance in the ejected-electron continuum, is expected to be small since the first such autoionising state is of the type $3s3p^5nl$ ($n \geq 4$), which has a small excitation cross section. Another additional contribution to single ionisation was already mentioned by Woodruff *et al*; ionisation of Ar^+ plus excitation of the resulting Ar^{2+} ion. Since this is due to a double electron interaction the cross section should also be small.

The broken curve in figure 8 is the binary encounter cross section for ionisation of Ar^+ calculated in the classical binary-encounter approximation (BEA, Gryzinski 1965)

$$\sigma = \sigma_0 \sum_i g_i(x) n_i / P_i^2 \tag{19}$$

where $x = E/P_i$ and for electron impact $\sigma_0 = 6.56 \times 10^{-14}$ cm^2 eV^2. The form of the

cross section is given by

$$g_i(x) = \frac{1}{x}\left(\frac{x-1}{x+1}\right)^{3/2}\left[1+\frac{2}{3}\left(1-\frac{1}{2x}\right)\ln[2.7+(x-1)^{1/2}]\right]. \tag{20}$$

n_i and P_i are the same as for equation (18). Also here the summation was extended only over the 3p and the 3s subshells. At energies above 200 eV the BEA nearly coincides with the Lotz formula and the two experiments. There are large discrepancies between BEA and the experimental points at energies below 70 eV which reflect the uncertainties involved in the semiclassical theory.

The best founded theoretical calculation is that of Younger (1982) represented by the chain curve. This quantum mechanical approach is mainly based on the distorted-wave theory including electron exchange (DWX). The DWX calculation (again for the 3p and 3s subshells only) shows good agreement with the experiments at electron energies below 40 eV. Deviations of about 25% occur above the energy of the cross section maximum. The DWX cross section agrees quite well with our previous experiment for Ar^+ ions (Müller *et al* 1980); however, those measurements were based on assumptions about the electron current density in the interaction region, and because of the inherent uncertainties had larger error bars.

The calculated cross sections discussed here are known to take into account only direct ionisation. The extent of agreement with the experiment is typical for cross sections for which indirect ionisation processes are negligible. Although Younger's calculation is one of the best quantum theoretical approaches presently available it deviates by about 25% from the present measurements and those of Woodruff *et al.* The Lotz formula once again gives a very good approach to the measured data. However, this is due to the dominance of the direct ionisation mechanism in process (17). In general, the accuracy of this semiempirical formula may be very uncertain especially for highly charged complex ions (see e.g. Falk *et al* 1981) since single ionisation may in some cases be dominated by far by excitation-autoionisation processes.

9. Conclusion

We have applied an improved technique to the measurement of independently absolute cross sections for electron impact ionisation of ions with crossed beams. Compared with the animated-beam technique of Brouillard and his co-workers the present method has the advantage of automatic parallel displacement of the electron beam across the ion beam. With the simultaneous measurement of the parent ion current as a function of the electron beam position it would even be possible to do measurements with the speed of the electron gun movement *not* constant. For this purpose, however, the problem of variable channel widths and noise on the voltage ramp V would have to be carefully considered. The new technique gives cross section results of a quality comparable with the well established static crossed-beams measurements with modulated beam intensities.

The actual measuring time for a cross section function like that for Ar^+ presented in figure 8 is now only about 6 h. Within reasonable time it would be possible therefore to accumulate a good deal of the knowledge about cross sections for electron impact ionisation of ions necessary to meet the data needs of the fusion community, provided that beams of the desired ions are available.

Acknowledgment

We would like to express our gratitude to Dr Ch Achenbach, H H Pitz and W Schneider for support and technical assistance. We also thank very much Dr H Baumann and Professor Dr K Bethge for the blueprints of their Penning ion source.

References

Achenbach C, Müller A, Salzborn E and Becker R 1984 *J. Phys. B: At. Mol. Phys.* **17** 1405-25
Baumann H and Bethge K 1981 *Nucl. Instrum. Meth.* **189** 107-10
Brouillard F and Claeys W 1983 *Physics of Ion-Ion and Electron-Ion Collisions* ed F Brouillard and J W McGowan (New York and London: Plenum) pp 415-59
Chen M H and Crasemann B 1974 *Phys. Rev.* **10** 2232-9
Clausnitzer G, Klinger H, Müller A and Salzborn E 1975 *Nucl. Instrum. Meth.* **128** 1-7
Clementi E and Roetti C 1974 *At. Data Nucl. Data Tables* **14** 177-478
Defrance P, Brouillard F, Claeys W and van Wassenhove G 1981 *J. Phys. B: At. Mol. Phys.* **14** 103-10
Falk R A, Dunn G H, Griffin D C, Bottcher C, Gregory D C, Crandall D H and Pindzola M S 1981 *Phys. Rev. Lett.* **47** 494-7
Gryzinsky M 1965 *Phys. Rev.* **138** A336-58
Harrison M F A 1968 *Methods of Experimental Physics* vol 7A ed B Bederson and W L Fite (New York: Academic) pp 95-115
Lotz W 1968 *Z. Phys.* **216** 241-7
Moore C E 1970 *Atomic Energy Levels* NSRDS-NBS 34 (Washington, DC: US Govt Printing Office)
Müller A and Frodl R 1980 *Phys. Rev. Lett.* **44** 29-32
Müller A and Salzborn E 1979 *Nucl. Instrum. Meth.* **164** 607-8
Müller A, Salzborn E, Frodl R, Becker R, Klein H and Winter H 1980 *J. Phys. B: At. Mol. Phys.* **13** 1877-99
Rinn K, Müller A, Eichenauer H and Salzborn E 1982 *Rev. Sci. Instrum.* **53** 829-37
Woodruff P R, Hublet M-C and Harrison M F A 1978 *J. Phys. B: At. Mol. Phys.* **11** L305-8
Younger S M 1982 *Phys. Rev.* A **25** 3396-8